

A new method for the experimental study of topological effects in the quark-gluon plasma

N. N. Ajitanand,¹ Roy A. Lacey,¹ A. Taranenko,¹ and J. M. Alexander¹

¹*Department of Chemistry, Stony Brook University,
Stony Brook, NY, 11794-3400, USA*

(Dated: August 26, 2018)

A new method is presented for the quantitative measurement of charge separation about the reaction plane. A correlation function is obtained whose shape is concave when there is a net separation of positive and negative charges. Correlations not specifically associated with charge, from flow, jets and momentum conservation, do not influence the shape or magnitude of the correlation function. Detailed simulations are used to demonstrate the effectiveness of the method for the quantitative measurement of charge separation. Such measurements are a pre-requisite to the investigation of topological charge effects in the QGP as derived from the “strong \mathcal{CP} problem”.

PACS numbers: Valid PACS appear here

INTRODUCTION

Topological charge fluctuations play an important role in the structure of the QCD vacuum [1]. It manifests in the breaking of chiral symmetry, as well as in the mass spectrum and other properties of hadrons. These fluctuations can also lead to the formation of metastable vacuum domains, especially in the vicinity of the de-confinement phase transition, in which fundamental symmetries (\mathcal{P} and/or \mathcal{CP}) are spontaneously broken [2] *i.e.* the so-called “strong \mathcal{CP} problem”. Experimental evidence for such topological fluctuations have been largely indirect.

Recently, it has been suggested that direct experimental signatures of topological fluctuations could result from quark gluon plasma (QGP) [quarks liberated from hadronic confinement] subjected to an intense (hadron-scale) external magnetic field, via the so called chiral magnetic effect (CME) [3, 4]. In brief, topological charge fluctuations in the QGP leads to an axial anomaly or local imbalance between left-handed and right-handed light quarks. In an intense magnetic field, these quarks move along the field to create a net electric current which results in a separation of positive and negative electric charges in the field direction. Evidence for the chiral magnetic effect has been found in recent numerical lattice QCD calculations [5]. An axial anomaly can also result from an anomalous global symmetry current in the hydrodynamic description of the QGP [6]. This results in a modification of the hydrodynamic current by a term proportional to the vorticity of the fluid, and manifests also as a separation of positive and negative electric charges perpendicular to the reaction plane. Hereafter, we term this as the chiral rotation effect (CRE).

MEASURING TOPOLOGICAL EFFECTS

Collisions between heavy nuclei at the Relativistic Heavy Ion Collider (RHIC), not only create a strongly

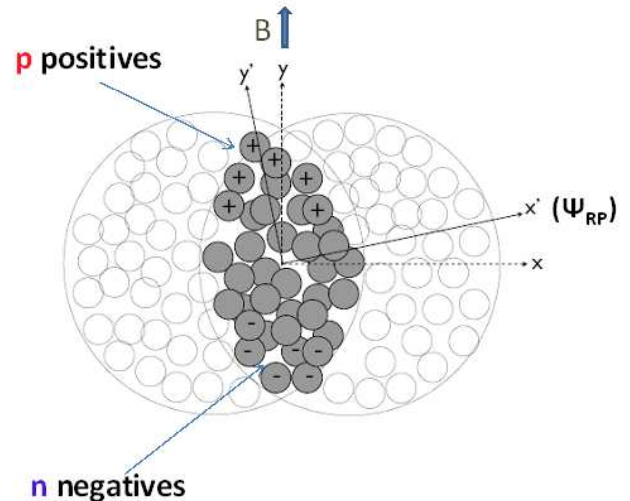


FIG. 1. Schematic illustration of the chiral magnetic effect. Colliding nuclei (depicted as circles) are moving in and out of the page respectively. The Magnetic field (B) and system orbital angular momentum (L) are perpendicular to the reaction plane (plane spanned by the impact parameter, b , and colliding nuclei direction). Note that the overlap zone is not necessarily aligned with B or L .

coupled low viscosity QGP [7–14] but also the strongest magnetic fields [orthogonal to the reaction plane] attainable in the laboratory [15]. Consequently, the chiral magnetic effect or the chiral rotation effect is expected to lead to a charge asymmetry in the distribution of particles emitted about the reaction plane (see Fig. 1). Experimental studies of such an asymmetry could provide an important avenue for investigating one of the most important problems of strong interaction theory.

The STAR collaboration has analyzed data from recent measurements of Au+Au and Cu+Cu collisions (at

55 $\sqrt{s_{NN}} = 200$ GeV) in search of this charge asymmetry
 56 with respect to the reaction plane. To do this they con-
 57 structed a correlator which used the emission angles of
 58 like-sign (+ + or - -) and opposite-sign (+ -) hadron
 59 pairs. The correlator is defined by the event average

$$C^{(\pm,\pm)} = \left\langle \cos(\phi_\alpha^{(\pm)} + \phi_\beta^{(\pm)} - 2\Psi_2) \right\rangle, \quad (1)$$

60 where ϕ_α, ϕ_β denote the azimuthal emission angles of any
 61 pair of hadrons, and Ψ_2 denotes the azimuthal orienta-
 62 tion of the estimated second order event plane. The dif-
 63 ference

$$\Delta Q \sim C^{(++)} + C^{(--)} - 2C^{(+-)} \quad (2)$$

64 was used to test for a charge separation [about the re-
 65 action plane] of the kind suggested by the CME and the
 66 CRE, after an appropriate correction for dispersion of the
 67 reaction plane.

68 A charge separation has been reported by the STAR
 69 collaboration [16, 17]. However, its mechanistic origin is
 70 still under intense debate [18–22]. One reason for this
 71 has been the observation that the correlator used in the
 72 STAR analysis may be sensitive to several well known
 73 “background” correlations such as elliptic flow, jets and
 74 momentum conservation [19, 21, 22]. Therefore, it is im-
 75 portant to develop and investigate new correlators which
 76 can overcome many, if not all, of these deficiencies.

77 A full study of topological effects in the QGP and its
 78 implications for the “strong \mathcal{CP} problem”, will undoubt-
 79 edly require further detailed measurements focused on
 80 accurate experimental quantification of the dependence
 81 of charge asymmetry on particle species, particle p_T ,
 82 collision-system deformation, event centrality and beam
 83 collision energy. Here, we present a new experimental
 84 correlator specifically designed to aid such investigations.
 85 Our technique involves a multi-particle charge-
 86 sensitive in-event correlator $C_c(\Delta S)$, which is expressed
 87 as a ratio of two distributions;

$$C_c(\Delta S) = \frac{N(\Delta S_{csep})}{N(\Delta S_{cmix})}. \quad (3)$$

88 The numerator is a distribution over events of the event
 89 averaged quantity ΔS_{csep} defined as

$$\Delta S_{csep} = \langle S_p^{h+} \rangle - \langle S_n^{h-} \rangle \quad (4)$$

90 where

$$\langle S_p^{h+} \rangle = \frac{\sum_1^p \sin(\Delta\varphi_+)}{p}, \quad \langle S_n^{h-} \rangle = \frac{\sum_1^n \sin(\Delta\varphi_-)}{n}, \quad (5)$$

91 n and p are the numbers of negative and positive hadrons
 92 [respectively] emitted about the observed event plane
 93 Ψ_{EP} ($m = n + p$ is the charge hadron multiplicity for
 94 an event) and $\Delta\varphi = \phi - \Psi_{EP}$ where ϕ is the azimuthal
 95 emission angle of the charged hadron.

96 The distribution ΔS_{cmix} in the denominator in Eq. 3,
 97 is obtained by making event averages in a slightly differ-
 98 ent way; That is, Eq. 5 is used to evaluate the averages
 99 $\langle S_p^h \rangle$ and $\langle S_n^h \rangle$ for p and n randomly chosen hadrons
 100 (irrespective of charge) i.e.

$$\Delta S_{cmix} = \langle S_p^h \rangle - \langle S_n^h \rangle. \quad (6)$$

101 There are several important features of the new cor-
 102 relator $C_c(\Delta S)$. First, it is constructed entirely from a
 103 real event; hence, it is pure in event class (centrality,
 104 vertex, etc). Second, it is rather insensitive to the back-
 105 ground correlations which influence reliable extraction of
 106 the magnitude of the charge-separation correlation (see
 107 discussion below). In what follows, we use detailed sim-
 108 ulations to demonstrate the expected trends, as well as
 109 the efficacy of $C_c(\Delta S)$.

SIMULATION METHODOLOGY

110 The response of $C_c(\Delta S)$ to a charge-separation signal
 111 was tested via a detailed set of simulations tuned to re-
 112 produce observed experimental features. The simulations
 113 included the following major steps for each event.

- The event plane was chosen at random from 2π . Charged particles were then emitted with an azimuthal distribution with respect to this reaction plane as:

$$N(\Delta\varphi) \propto (1 + 2v_2 \cos \Delta\varphi) + 2v_4 \cos(4\Delta\varphi) + 2a_1 \sin(\Delta\varphi), \quad (7)$$

where the Fourier coefficients v_2 and v_4 are the observed magnitudes of elliptic and hexadecapole flow, and a_1 is the charge-separation signal of interest. The number and p_T distribution of particles were tuned to match the experimentally observed distributions. The reaction plane was then dispersed according to the experimentally observed dispersion for the centrality selection under study.

- Neutral decay particles (e.g. Λ and K_0) were emitted with respect to the reaction plane according to their observed flow patterns. The decay kinematics of these resonances were followed so as to obtain the daughter particle directions and momenta. The relative abundance of the decay particles were constrained by the requirement that the simulated and observed positive-negative charge pair correlations (obtained by the standard event mixing method) were in agreement.
- Jet particles were emitted with respect to the jet axes in a manner which was consistent with the observed two-particle jet correlations.

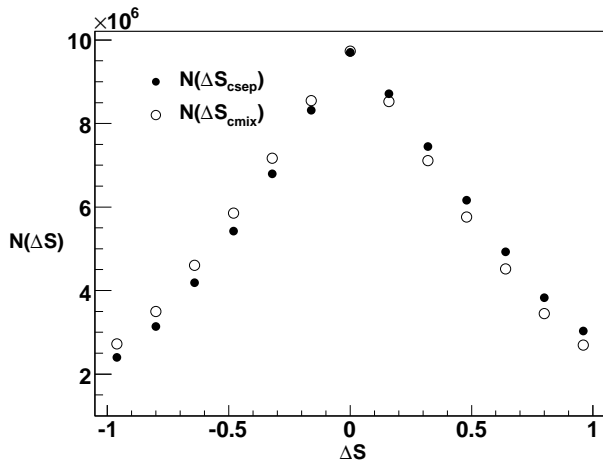


FIG. 2. $N(\Delta S)_{csep}$ and $N(\Delta S)_{cmix}$ distributions for simulations performed with $a_1 > 0$ for all events.

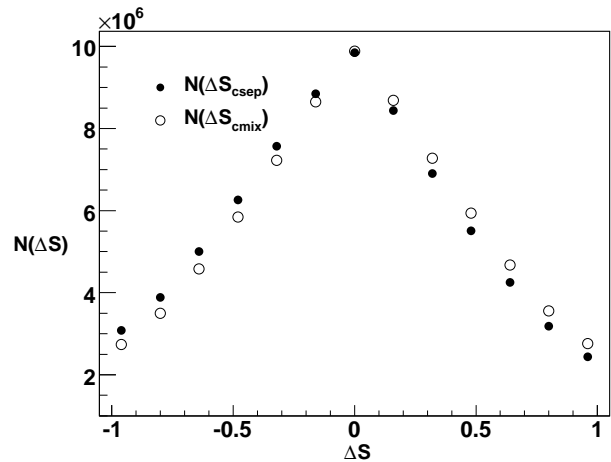


FIG. 3. $N(\Delta S)_{csep}$ and $N(\Delta S)_{mix}$ distributions for simulations performed with $a_1 < 0$ for all events.

- 140 • All emitted particles were passed through an acceptance filter specifically designed to take account of the detector acceptance and consequently, reproduce the measured inclusive distributions for positive and negative hadrons respectively as a function of p_T .
- 141
- 142
- 143
- 144
- 145
- 146 • The simulated events were analyzed as if they were actual experimental events. The correlation $C_c(\Delta S)$ was evaluated for the selected range of p_T using the detected particles and the dispersed reaction planes using Eqs. 3 - 6.
- 147
- 148
- 149
- 150

151 RESULTS FROM SIMULATIONS

152 Simulations were performed for a broad spectrum of
 153 scenarios. Here, we show a representative set of results
 154 which lends insight into the detailed nature of $C_c(\Delta S)$, as
 155 well as its sensitivity to different sources of background
 156 correlations.

157 The distributions for $N(\Delta S)_{csep}$ (solid circles) and
 158 $N(\Delta S)_{mix}$ (open circles) are compared in Figs. 2 and
 159 3 for $a_1 > 0$ and $a_1 < 0$ (respectively) for all events.
 160 Fig. 2 shows that for $a_1 > 0$ the distribution for
 161 $N(\Delta S)_{csep}$ is shifted to the right when compared to that
 162 for $N(\Delta S)_{mix}$. Similarly Fig. 3 shows that for $a_1 < 0$,
 163 the distribution for $N(\Delta S)_{csep}$ is shifted to the left when
 164 compared to that for $N(\Delta S)_{mix}$. Figs. 4 and 5 show
 165 the respective $C_c(\Delta S)$ distributions which result from the
 166 ratio of the distributions shown in Figs. 2 and 3. They
 167 indicate sizable deviations from a flat distribution with
 168 positive and negative slopes respectively. Note that a flat
 169 distribution would be indicative of no charge-separation.
 170 $C_c(\Delta S)$ distributions are shown in Figs. 6 and 7 for sim-
 171 ulated events in which (i) 51% of the events were gener-
 172 ated with $a_1 > 0$ and the other 49 % with $a_1 < 0$, and

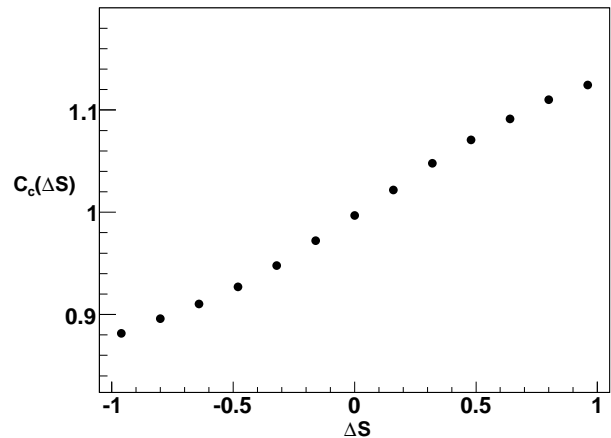


FIG. 4. Distribution for $C_c(\Delta S)$ obtained from the ratio of the distributions shown in Fig. 2.

- 175 (ii) 49% of the events with $a_1 > 0$ and 51% of the events
 176 with $a_1 < 0$. In both cases, an asymmetric concave dis-
 177 tribution is obtained but with opposite asymmetry.

178 The distributions for $N(\Delta S)_{csep}$ and $N(\Delta S)_{mix}$ ob-
 179 tained for a simulation in which 50% of the events were
 180 generated with $a_1 > 0$ and the other 50% with $a_1 < 0$
 181 are shown in Fig. 8. This choice was made to mimic the
 182 effects of local parity violation implied by current mod-
 183 els of topological charge generation in the QGP. For this
 184 scenario, Fig. 8 indicates that although the two distribu-
 185 tions are strikingly similar, $N(\Delta S)_{csep}$ is slightly broader
 186 than $N(\Delta S)_{mix}$. This is made more transparent in Fig.9
 187 by the symmetric concave shape obtained for $C_c(\Delta S)$
 188 from the ratio of these distributions.

189 To investigate the influence of “background” correla-
 190 tions from flow, jets and resonance decays, several sim-
 191 ulations were performed with these correlations turned

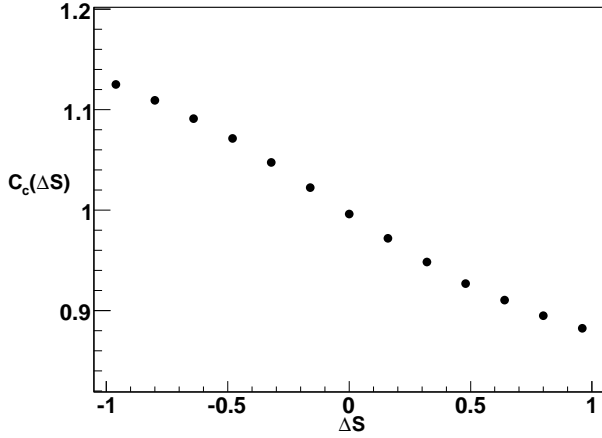


FIG. 5. $C_c(\Delta S)$ correlation function obtained from the ratio of the distributions shown in Fig. 3.

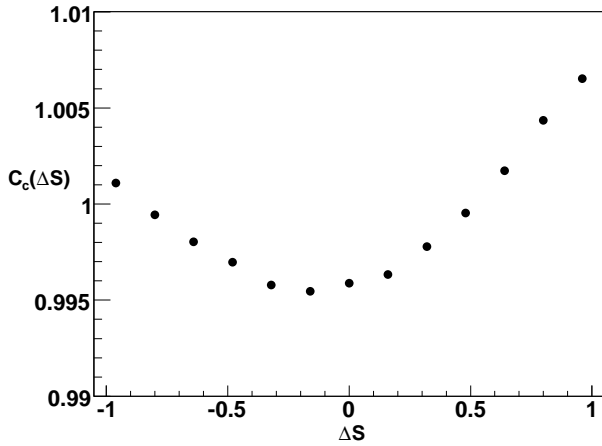


FIG. 6. $C_c(\Delta S)$ correlation function obtained with $a_1 > 0$ in 51% of events and $a_1 < 0$ in 49% of events.

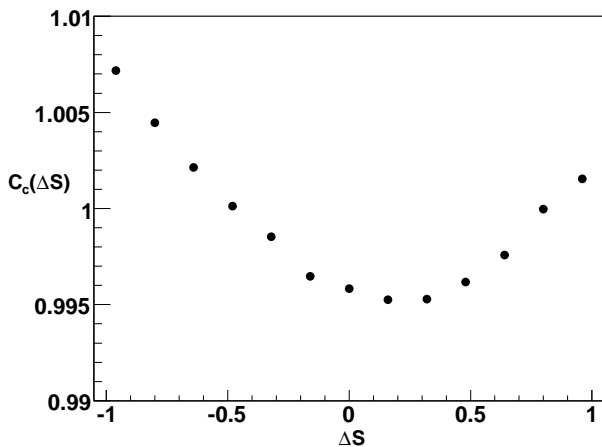


FIG. 7. $C_c(\Delta S)$ correlation function obtained with $a_1 > 0$ in 49% of events and $a_1 < 0$ in 51% of events.

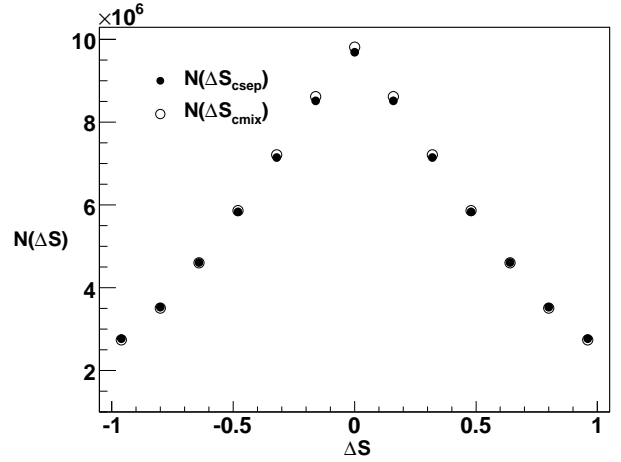


FIG. 8. Comparison of $N(\Delta S)_{csep}$ and $N(\Delta S)_{mix}$ distributions for simulations performed with $a_1 < 0$ in 50% of the events and $a_1 > 0$ in the other 50%.

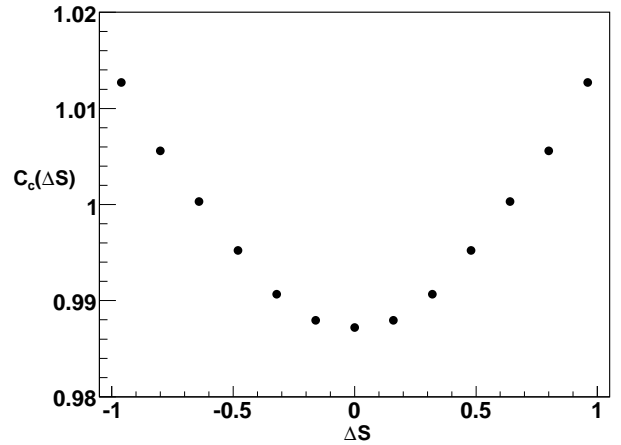


FIG. 9. $C_c(\Delta S)$ correlation function obtained from the ratio of the distributions shown in Fig. 8.

192 on or off. Fig. 10 shows the correlation function for a
 193 simulation in which only flow correlations are turned on
 194 for all events, i.e. $v_{2,4} \neq 0$, $a_1 = 0$ and resonance de-
 195 cays are turned off. The flat distribution indicated by
 196 Fig. 10 shows that $C_c(\Delta S)$ is insensitive to flow. In
 198 contrast to Fig. 10, Fig. 11 shows a convex shape for
 199 $C_c(\Delta S)$ which results from the charge correlations associ-
 200 ated with resonance decays which tends to bring opposite
 201 charges closer together in azimuth than on average. For
 202 this correlation function, the simulation was performed
 203 with flow on, $a_1 = 0$ and resonance decays on, for all
 204 events. Since these correlations have an opposite influ-
 205 ence on the shape of $C_c(\Delta S)$ [compared to that for the
 206 charge separation signal], it is important to have the rela-
 207 tive abundances of decay particles properly incorporated
 208 into the simulations. This is ensured by requiring the

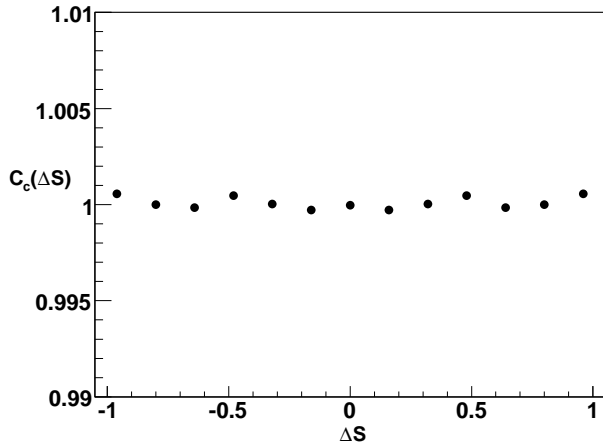


FIG. 10. $C_c(\Delta S)$ correlation function obtained for simulated events with only flow correlations.

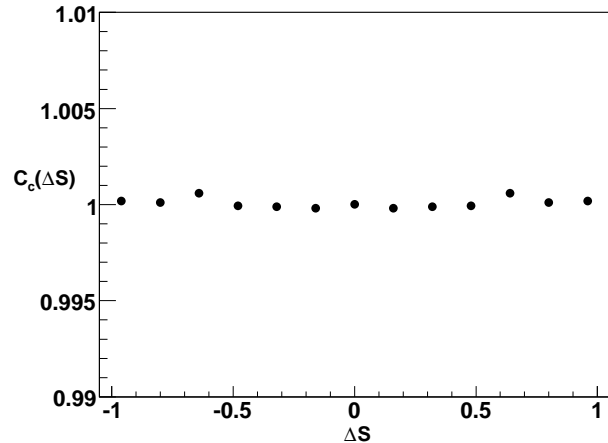


FIG. 12. $C_c(\Delta S)$ correlation function obtained for simulated events with jets on, flow on, no resonance decay and $a_1=0$.

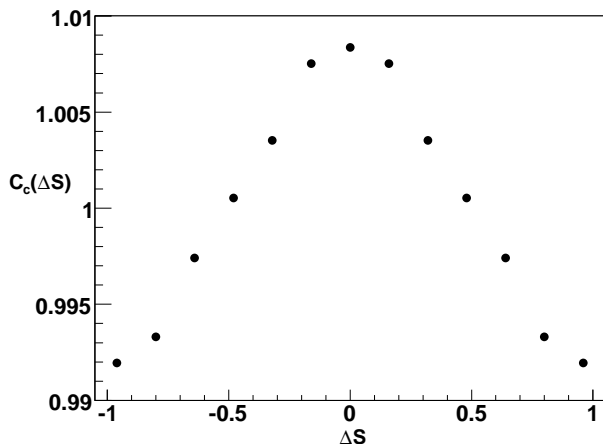


FIG. 11. $C_c(\Delta S)$ correlation function obtained for simulated events with flow on, resonance decay on and $a_1 = 0$.

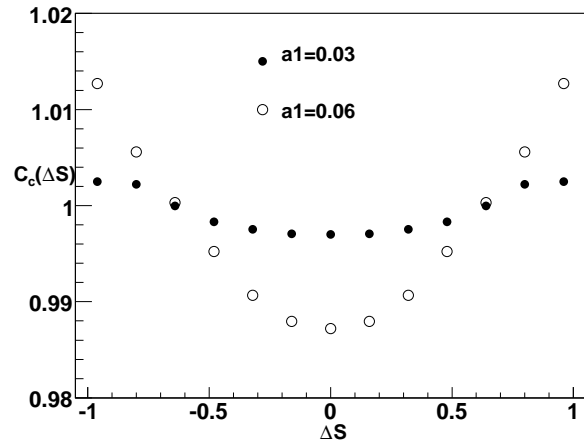


FIG. 13. $C_c(\Delta S)$ correlation functions obtained for simulated events with $a_1=0.03$ and $a_1=0.06$.

209 standard two particle opposite charge correlations from
210 the simulations to match those for experimental data.

212 The correlation function shown in Fig. 12 was obtained
213 for simulated events in which flow is on, $a_1 = 0$, resonance
214 decays are off, but jets are turned on for all events. It is
215 very similar to the flat distribution seen in Fig. 10 and
216 confirms the absence of any significant background cor-
217 relations to $C_c(\Delta S)$ from jets. Because the same event
218 is used to construct both $N(\Delta S)_{csep}$ and $N(\Delta S)_{mix}$ mo-
219 mentum correlation effects are also not expected to play
220 any significant role.

221 For an actual experimental correlation signal, the value
222 of a_1 would be obtained by matching simulation to the
223 observed correlation. The sensitivity of $C_c(\Delta S)$ to the
224 the parameter used to specify the magnitude of the
225 charge separation a_1 is demonstrated in Fig. 13. It
226 shows that $C_c(\Delta S)$ is responsive even to a relatively small

227 charge asymmetry.

228 It is important to stress that the method presented
229 here is very general. For this study it has been applied
230 to the correlations between charges in an event. However,
231 our methodology can be applied to the investigation of
232 correlations within any observed particle property.

233 SUMMARY

234 In summary, we have presented a new method which
235 allows for good quantitative measurement of charge sep-
236 aration about the reaction plane. Our method involves
237 the formulation of a novel correlation function $C_c(\Delta S)$
238 whose shape is concave only when there is a non-zero
239 charge separation signal. The strength of $C_c(\Delta S)$ is re-
240 lated to the parameter a_1 which can be linked to a parity

241 violating signal. It is noteworthy that experimentally a
 242 reaction plane obtained from second order flow (v_2) has
 243 a $\pm\pi$ ambiguity. Introduction of such an ambiguity in
 244 the simulations makes all correlations symmetric i.e. the
 245 sensitivity to global parity violation would be lost since
 246 the sign of a_1 cannot be determined. However the sensi-
 247 tivity of the correlation function to the magnitude of a_1
 248 remains. Correlations due to flow, jets and momentum
 249 conservation, do not influence the shape nor the magni-
 250 tude of $C_c(\Delta S)$. Therefore, $C_c(\Delta S)$ measurements could
 251 provide an important framework for investigating one of
 252 the most important problems of strong interaction theory
 253 – the “strong \mathcal{CP} problem”.

254 [1] T. Schafer and E. V. Shuryak, *Rev. Mod. Phys.* **70**, 323
 255 (1998), [arXiv:hep-ph/9610451](#).
 256 [2] D. E. Kharzeev, *Annals Phys.* **325**, 205 (2010),
 257 [arXiv:0911.3715 \[hep-ph\]](#).
 258 [3] D. Kharzeev, *Phys. Lett.* **B633**, 260 (2006), [arXiv:hep-](#)
 259 [ph/0406125](#).
 260 [4] K. Fukushima, D. E. Kharzeev, and H. J. Warringa,
 261 *Nucl. Phys.* **A836**, 311 (2010), [arXiv:0912.2961 \[hep-ph\]](#).
 262 [5] P. V. Buividovich, M. N. Chernodub, E. V.
 263 Lushevskaya, and M. I. Polikarpov, *Phys. Rev.*
 264 **D81**, 036007 (2010), [arXiv:0909.2350 \[hep-ph\]](#).
 265 [6] D. T. Son and P. Surowka, *Phys. Rev. Lett.* **103**, 191601
 266 (2009), [arXiv:0906.5044 \[hep-th\]](#).

[7] K. Adcox *et al.* (PHENIX), *Nucl. Phys.* **A757**, 184
 (2005), [arXiv:nucl-ex/0410003](#).
 [8] R. A. Lacey *et al.*, *Phys. Rev. Lett.* **98**, 092301 (2007),
[arXiv:nucl-ex/0609025](#).
 [9] M. Luzum and P. Romatschke, *Phys. Rev.* **C78**, 034915
 (2008).
 [10] H. Song and U. W. Heinz, *J. Phys.* **G36**, 064033 (2009).
 [11] A. K. Chaudhuri, (2009), [arXiv:0910.0979 \[nucl-th\]](#).
 [12] R. A. Lacey, A. Taranenko, and R. Wei, (2009),
[arXiv:0905.4368 \[nucl-ex\]](#).
 [13] G. S. Denicol, T. Kodama, and T. Koide, (2010),
[arXiv:1002.2394 \[nucl-th\]](#).
 [14] R. A. Lacey *et al.*, (2010), [arXiv:1005.4979 \[nucl-ex\]](#).
 [15] J. Rafelski and B. Muller, *Phys. Rev. Lett.* **36**, 517
 (1976).
 [16] B. I. Abelev *et al.* (STAR), *Phys. Rev. Lett.* **103**, 251601
 (2009), [arXiv:0909.1739 \[nucl-ex\]](#).
 [17] B. I. Abelev *et al.* (STAR), *Phys. Rev.* **C81**, 054908
 (2010), [arXiv:0909.1717 \[nucl-ex\]](#).
 [18] M. Asakawa, A. Majumder, and B. Muller, *Phys. Rev.*
C81, 064912 (2010), [arXiv:1003.2436 \[hep-ph\]](#).
 [19] A. Bzdak, V. Koch, and J. Liao, (2010), [arXiv:1008.4919](#)
[\[nucl-th\]](#).
 [20] B. Muller and A. Schafer, (2010), [arXiv:1009.1053 \[hep-](#)
 291 [ph\]](#).
 [21] F. Wang, *Phys. Rev.* **C81**, 064902 (2010),
 292 [arXiv:0911.1482 \[nucl-ex\]](#).
 [22] S. Schlichting and S. b. e. Pratt, (2010), [arXiv:1005.5341](#)
 293 [\[nucl-th\]](#).